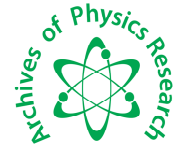




## Scholars Research Library

Archives of Physics Research, 2011, 2 (3):1-11  
(<http://scholarsresearchlibrary.com/archive.html>)



Scholars Research  
Library

ISSN : 0976-0970

CODEN (USA): APRRC7

### Generation of obliquely propagating Whistler mode instability for inhomogeneous ionospheric plasma

<sup>1</sup>R. S. Pandey, <sup>2</sup>H. Singh, J. Kishor N. K. Pandey and S. Md. Karim, <sup>3</sup>Pramod Kumar

<sup>1</sup>Department of Physics, Amity School of Engineering & Technology, Amity University, Noida(U. P.), India

<sup>2</sup>Department of Physics, Veer Kunwar Singh University, Ara, Bihar, India

<sup>3</sup>Department of Physics, J. L. N. College Chakradharpur Ranchi University Ranchi, Jharkhand, India

---

#### ABSTRACT

*Whistler mode instability having propagation vector oblique to ambient magnetic field has been studied for pitch angle loss-cone unperturbed distribution function for inhomogeneous ionospheric plasma. Dispersion relation and growth rate have been derived and calculated for ionospheric plasma having inhomogeneity in perpendicular AC electric field, loss-cone and temperature anisotropy. The growth rate of electromagnetic circularly polarized VLF wave has been founded to be enhanced by free energy source like temperature anisotropy and loss-cone up to a limited angle of propagation. It is also inferred that perpendicular AC electric field modifies the resonance frequency condition.*

**Key words:** Obliquely propagating whistler, Ionosphere.

---

#### INTRODUCTION

Electrons can be scattered into the Loss-cone by wave particle interaction between whistler mode radiation and energetic electrons in the magnetosphere. The whistler mode radiation responsible for this pitch angle diffusion may take the form of either incoherent or coherent emissions. Incoherent whistler mode radiation can result from instabilities driven by anisotropies in the velocity distribution of the hot electrons [1, 2]. Coherent whistler emissions can result from phase bunching of energetic electrons triggered by external emissions or by incoherent whistler waves [3]. The scattering electron into the loss-cone by incoherent whistler radiation was considered by Kennel and Petschek[4], while the pitch angle scattering caused by coherent whistler emissions was treated by Inan et al [5]. Whistler waves are believed to play an important role in the generation of the pulsating aurora. It is now firmly established that the glow of the pulsating aurora is caused by the quasi-periodic filling of the loss-cone and the subsequent

precipitation of energetic electrons into the atmosphere [6]. Based on electron energy measurements obtained from sounding rockets experiments, the scattering mechanism is believed to occur in the equatorial plane. The ionosphere is believed to play some role in determining the spatial characteristics of the pulsating aurora because the drift rate of the auroral patches appears to be related to the movement of the neutral atmosphere [7]. Oguti [8] proposed that local enhancements in the ionospheric plasma density may explained to fill adjacent flux tubes with different plasma densities, there by creating the conditions needed at the equator to trigger auroral pulsations.

Huang et al [9] calculated the characteristics of the incoherent whistler mode waves generated in the magnetosphere along the  $L = 5$  geomagnetic field line which intersect the atmosphere in the region where the pulsating aurora is frequently observed and considered their implications for the pulsating aurora. They observed for the loss-cone driven Whistler instability, the growth rate along the  $L = 5$  field line in largest just above the ionosphere where the loss-cone angle is also large.

A spatially distributed mode current of Whistler wave oscillating at the modulation frequency of the ground transmitted powerful HF wave can be induced in the E-region of the high-latitude ionosphere through the coupling between HF wave modulated electro jet current and induced density irregularities. These density irregularities generated by the HF wave via a thermal instability vary periodically along the geomagnetic field. This current produces whistler waves directly rather than through an antenna radiation process. This mechanism generates whistler waves in the VLF range (3-30keV) with reduced harmonic components. The frequencies of produced whistler waves depend on the Polarization, frequency, power and modulation scheme of the HF wave .It is predicted that whistler waves at frequency around 25KHz.can be most favorably excited. During sub storm expansion, strong stimulated electromagnetic emission (SEE) at the harmonic of the down shifted maximum frequency has been found. It is believed that SEE is accompanied by excitation of the VLF waves penetrating into magnetosphere and stimulating the precipitation of the energetic electrons (10-40KeV) of 1-min duration due to cyclotron resonant interaction of the natural precipitation electrons (1-10KeV) with the heater-induced whistler waves in the magnetosphere. In the recovery phase of the auroral sub storm emissions at the heater second harmonics frequency was the large decay time up to several minutes after the heater turn-off. The possible explanation for these emissions can be found from the linear conversion process when the pump wave of O-mode may directly convert to electrostatic waves in the region of the HF plasma resonance .The large decay time may result from electromagnetic instability growth in the heater – modified ionosphere at the downward field-aligned currents.

Strong variations of auroral hiss intensity and cut off frequency correlating with auroral dynamics were observed well pole ward from the auroral oval. The auroral hiss intensity bursts correlated with intensifications of aurora arcs as well as with magnetic disturbances. The cut off frequency of auroral hiss depends on the distance decreases and vice-versa. Such behavior of cut off frequency can be explained by propagation in the Whistler mode at wave normal angles near the resonance cone from a moving spatially localized source.

In this paper Whistler mode instability having propagation vector to ambient magnetic field has been studied for pitch angle loss-cone unperturbed distribution function for inhomogeneous ionospheric plasma. Dispersion relation and growth rate have been derived and calculated for ionospheric plasma having in homogeneity in perpendicular AC electric field, loss-cone and temperature anisotropy. The growth rate of electromagnetic circularly polarized VLF wave has been found to be enhanced by free energy source like temperature anisotropy and loss-cone up to a limited angle of propagation. It is also inferred that perpendicular AC electric field modifies the resonance frequency condition.

## II. Dispersion Relation

A spatially homogeneous an isotropic, collision less magneto plasma subjected to an external magnetic field  $B_0 = B_0 e_x$  and an electric field  $E_0 = (E_0 \sin v t \hat{e}_x)$  has been considered in order to obtain the relation. In case, the Vlasov-Maxwell equations are linearized. The linearized equations obtained after neglecting the higher order terms and separating the equilibrium and non-equilibrium parts, following the techniques of Pandey et al [10, 11] are given as

$$v \frac{\partial f_{s0}}{\partial r} + \frac{e_s}{m_s} [E_0 \sin v t + (v \times B_0)] \left( \frac{\partial f_{s0}}{\partial v} \right) = 0 \quad \dots(1)$$

$$\frac{\partial f_{s1}}{\partial t} + v \cdot \frac{\partial f_{s1}}{\partial r} + \left( \frac{F}{m_s} \right) \left( \frac{\partial f_{s1}}{\partial v} \right) = S(r, v, t) \quad \dots(2)$$

where force is defined as  $F = m dv/dt$

$$F = e_s [E_0 \sin(v \times B_0)] \quad \dots(3)$$

The practical trajectories are obtained by solving the equation of motion defined in equ.(3) and  $S(r,v,t)$  is defined as.

$$\begin{aligned} x_0 &= x + \left( \frac{v_y}{\omega_{cs}} \right) + \left( \frac{1}{\omega_{cs}} \right) [v_x \sin \omega_{cs} t' - v_y \cos \omega_{cs} t'] + \left( \frac{\Gamma_x}{\omega_{cs}} \right) \left[ \frac{\omega_{cs} \sin v t' - v \sin \omega_{cs} t'}{\omega_{cs}^2 - v^2} \right] \\ y_0 &= y + \left( \frac{v_x}{\omega_{cs}} \right) - \left( \frac{1}{\omega_{cs}} \right) [v_x \cos \omega_{cs} t' - v_y \sin \omega_{cs} t'] - \left( \frac{\Gamma_x}{v \omega_{cs}} \right) \left[ 1 + \frac{v^2 \cos \omega_{cs} t' - \omega_{cs}^2 \cos v t'}{\omega_{cs}^2 - v^2} \right] \\ z_0 &= z - v_z t' \end{aligned} \quad \dots(4)$$

and the velocities are

$$v_{x0} = v_x \cos \omega_{cs} t' - v_y \sin \omega_{cs} t' + \left\{ \frac{v \Gamma_x (\cos v t' - \cos \omega_{cs} t')}{\omega_{cs}^2 - v^2} \right\}$$

$$v_{y0} = v_x \sin \omega_{cs} t' + v_y \cos \omega_{cs} t' - \left\{ \frac{\Gamma_x (\omega_{cs} \sin \omega_{cs} t' - v \sin \omega_{cs} t')}{\omega_{cs}^2 - v^2} \right\}$$

$$v_{z0} = v_z \tag{5}$$

where  $\omega_{cs} = \frac{e_s B_0}{m_s}$  is the cyclotron frequency of species  $s$  and  $\Gamma_x = \frac{e_s E_0}{m_s}$  and a.c. electric field is varying as  $E = E_{0x} \sin vt$ ,  $v$  being the angular a-c frequency.

$$S(r, v, t) = \left( -\frac{e_s}{m_s} \right) [E_1 + v \times B_1] \left( \frac{\partial f_{s0}}{\partial v} \right) \tag{6}$$

where  $s$  denotes species and  $E_1, B_1$  and  $f_{s1}$  are perturbed and are assumed to have harmonic dependence in  $f_{s1}, B_1$  and  $E_1 \sim \exp I(k, r - \omega t)$ . The method of characteristic solution is used to determine the perturbed distribution function  $f_{s1}$ , which is obtained from eq. (2) by

$$f_{s1}(r, v, t) = \int_{t_0}^{\infty} S(r_0(r, v, t), v_0(r, v, t), t - t_0) dt \tag{7}$$

The phase space coordinate system has been transformed from  $(r, v, t)$  to  $(r_0, v_0, t_0)$ . The particle trajectories which have been obtained by solving eq.(3) for the given external field configuration and wave propagation  $k = [k_{\perp} e_x, 0, k_{\parallel} e_z]$ . After doing some lengthy algebraic simplification and carrying out the integration, the perturbed distribution function  $f_1$  is written as [12]

$$f_{s1}(r, v, t) = -\frac{e_s}{m_s \omega} \sum_{m, n, p, q} \frac{J_p(\lambda_2) J_m(\lambda_1) J_q(\lambda_3) e^{i(k \cdot r - \omega t)}}{[\omega - k_{\parallel} v_{\parallel} - (n + q) \omega_{cs} + pv]} \left[ E_{1x} J_n J_p \left\{ \left( \frac{n}{\lambda_1} \right) U^* + D_1 \left( \frac{p}{\lambda_2} \right) \right\} \right. \\ \left. - i E_{1y} \left\{ J_n J_p C_1 + J_n J_p D_2 \right\} + E_{1z} J_n J_p W^* \right]$$

where the Bessel identity

$$e^{i\lambda \sin \theta} = \sum_{k=-\infty}^{\infty} J_k(\lambda) e^{ik\theta}$$

has been used, the arguments of the Bessel functions are

$$\lambda_1 = \frac{k_{\perp} v_{\perp}}{\omega_{cs}}, \lambda_2 = \frac{k_{\perp} \Gamma_x v}{\omega_{cs}^2 - v^2}, \lambda_3 = \frac{k_{\perp} \Gamma_x \omega_{cs}}{\omega_{cs}^2 - v^2}$$

where

$$C_1 = \frac{1}{v_{\perp}} \left( \frac{\partial f_0}{\partial v_{\perp}} \right) (\omega - k_{\parallel} v_{\parallel}) + \left( \frac{\partial f_0}{\partial v_{\parallel}} \right) k_{\parallel}$$

$$\begin{aligned}
 U^* &= C_1 \left[ v_{\perp} - \left\{ \frac{v\Gamma_x}{\omega_{cs}^2 - v^2} \right\} \right] \\
 W^* &= \left[ \left( \frac{n\omega_{cs}v_{\parallel}}{v_{\perp}} \right) \left( \frac{\partial f_0}{\partial v_{\perp}} \right) - n\omega_{cs} \left( \frac{\partial f_0}{\partial v_{\parallel}} \right) \right] + \left[ 1 + \left\{ \frac{k_{\perp}v\Gamma_x}{\omega_{cs}^2 - v^2} \right\} \left\{ (p/\lambda_2) - (n/\lambda_1) \right\} \right] \\
 D_1 &= C_1 \left\{ \frac{v\Gamma_x}{\omega_{cs}^2 - v^2} \right\}, D_2 = C_2 \left\{ \frac{\omega_{cs}\Gamma_x}{\omega_{cs}^2 - v^2} \right\} \\
 J'_n &= \frac{dJ_n(\lambda_1)}{d\lambda_1}, J'_p = \frac{dJ_p(\lambda_2)}{d\lambda_2} \qquad \dots(8)
 \end{aligned}$$

Following Pandey et al [11] the conductivity tensor  $\|\sigma\|$  is written as

$$\|\sigma\| = -\sum \frac{e_s^2}{m_s \omega_{n,n,p,q}} \sum \int \frac{J_q(\lambda_3) S_{ij} d^3v}{\omega - kv - (n+q)\omega_{cs} + pv}$$

where

$$S_{ij} = \begin{vmatrix} v_{\perp} \frac{n}{\lambda_1} (J_n)^2 J_p A & i v_{\perp} J_n B & v_{\perp} W^* \frac{n}{\lambda_1} J_n^2 J_p \\ v_{\perp} J_p A J_n J'_n & v_{\perp} J'_n B & i v_{\perp} W^* J_p J_n J'_n \\ v_{\parallel} J_n^2 J_p A & -i v_{\parallel} J_n B & v_{\parallel} W^* J_n^2 J_p \end{vmatrix}$$

$$A = \left( \frac{n}{\lambda_1} \right) U^* + \left( \frac{p}{\lambda_2} \right) D_1, \qquad B = J'_n J_p C_1 + J'_n J_n D_2$$

From  $J = \|\sigma\| E_1$  and two Maxwell's curl equations for the perturbed quantities, we have

$$\left[ k^2 - k.k - \frac{\omega^2}{c^2} \epsilon(k, \omega) \right] E_1 = 0$$

where

$$\epsilon(k, \omega) = 1 - \frac{4\pi}{i\omega} \|\sigma(k, \omega)\| \text{ is dielectric tensor}$$

The Maxwellian distribution function with loss-cone angle  $\theta_c$  taken from Huang et al [9] is written as

$$f_{so} = \frac{n_0}{M\pi^{3/2}\alpha_{\perp}^2\alpha_{\parallel}} \exp\left[-\left(\frac{v_{\perp}}{\alpha_{\perp}}\right)^2 - \left(\frac{v_{\parallel}}{\alpha_{\parallel}}\right)^2\right] \quad \left|\frac{v_{\perp}}{v_{\parallel}}\right| > \tan\theta_c$$

where normalization constant M is given as

$$M = \frac{1}{\sqrt{\frac{1 + \tan^2\theta_c}{A_T + 1}}}$$

$$\|\epsilon_{ij}(k, \omega)\| = 1 + \sum \frac{4\pi\pi_s^2}{m_s\omega^2} \int \frac{J_q(\lambda_3)\|S_{ij}\|d^3v}{\omega - kv - (n + q)\omega_{cs} + pv}$$

The generalized dielectric tensor may be written as

$$\left\| \begin{array}{ccc} N^2\cos^2\theta_1 + \epsilon_{11} & \epsilon_{12} & N^2\cos\theta_1\sin\theta_1 + \epsilon_{13} \\ \epsilon_{21} & N^2\epsilon_{22} & \epsilon_{23} \\ N^2\cos\theta_1\sin\theta_1 + \epsilon_{31} & \epsilon_{33} & N^2\sin^2\theta_1 + \epsilon_{33} \end{array} \right\|$$

If we remove the contribution of AC electric field and set normalization constant M=1 above dielectric tensor is similar to Sazhin [13] and Misra and Pandey [14]. After using the limits  $k_{\perp} = k\sin\theta_1 \rightarrow 0$  and  $k_{\parallel} = k\cos\theta_1$  the generalized dielectric tensor becomes simplified tensor and dispersion relation reduce as

$$\left\| \begin{array}{ccc} -N^2 + \epsilon_{11} & \epsilon_{12} & 0 \\ -\epsilon_{21} & -N^2 + \epsilon_{22} & 0 \\ 0 & 0 & \epsilon_{33} \end{array} \right\|$$

This is rewritten in more convenient form. Now for whistler wave

$$-N^4 - 2\epsilon_{11}N^2 + \epsilon_{11}^2 + \epsilon_{12}^2 = 0$$

for electrostatic waves  $\epsilon_{33} = 0$

Neglecting the higher power of N the resulting relation becomes as

$$\epsilon_{11} \pm \epsilon_{12} = N^2$$

Now the dispersion relation of oblique whistler wave is obtained from above for  $n = 1, p = 1$  and  $J_p = 1, J_q = 1$

$$\frac{k^2 c^2}{\omega^2} = 1 + \frac{\omega_p^2}{\omega^2} \left[ \left( 1 + \frac{X_{ac}}{\alpha_{\perp}} \right) \left\{ \frac{\omega}{Mk_{\parallel} \alpha_{\parallel}} Z(\xi + A_T (1 + \xi Z(\xi))) \right\} + \tan^2 \theta_c \right. \\ \left. \left\{ \left( \frac{1}{2} \right) + \xi^2 \left( 1 + \xi Z(\xi) + \frac{X_{ac}}{\alpha_{\perp}} \xi (1 + \xi Z(\xi)) \right) \right\} \right]$$

where

$$X_{ac} = \frac{v \Gamma_x}{\omega_c^2 - v^2} \quad X_3 = \frac{\omega_r}{\omega_c} \quad X_4 = \frac{-v}{\omega_c} \quad k_3 = 1 - X_3 + X_4, \quad k_4 = \frac{X_3}{k_3}$$

$$k_{\parallel} = k$$

The required expression for growth rate and real frequency are obtained as

$$\frac{\gamma}{\omega_c} = \frac{\sqrt{\lambda} \left[ \left( 1 + \frac{X_{ac}}{\alpha_{\perp}} \right) (A_T - k_4) + \left( \frac{\tan \theta_c k_3}{Mk} \right)^2 - \frac{X_{ac} \tan^2 \theta_c k_3}{\alpha_{\perp} Mk_{\parallel}} \right] k_3^3 \exp \left( - \left( \frac{k_3}{Mk_{\parallel}} \right) \right)}{\left( 1 + \frac{X_{ac}}{\alpha_{\perp}} \right) \left\{ 1 + X_4 \frac{M^2 A_T (1 + X_4)}{2k_3^2} - \frac{M^2 k_{\parallel}^2}{k_3} (A_T - k_4) \right\} + \frac{X_{ac} \tan^2 \theta_c}{2\alpha_{\perp}}}$$

$$X_3 = \frac{k_{\parallel}^2}{2\beta} \left[ 1 + X_4 \frac{M^2 A_T \beta \left( 1 + \frac{X_{ac}}{\alpha_{\perp}} \right)}{(1 + X_4)^2} + \frac{X_{ac} \tan^2 \theta_c M}{2\alpha_{\perp} k_{\parallel} (1 + X_4)} \right]$$

where

$$\beta = \frac{k_{\beta} T_{\parallel} n_0 \mu_0}{B_0^2}$$

### RESULTS AND DISCUSSION

Following plasma parameters studied to the aroral ionosphere has been adopted for the calculation of the growth rate and the real frequency for the loss-cone Driven Whistler instability. Ambient magnetic field  $B_0 = 1 \times 10^{-7} T$ , electron density  $n_0 = 1 \times 10^9 \text{ m}^{-3}$  electron energy  $K_B T_{11} = 10 \text{ eV}$ . Temperature anisotropy  $A_T$  is supposed to vary from 0.25 to 0.75 and loss-cone angle  $\theta^0_c$  is to vary from 0 to  $20^0$ . AC electric field has been considered equal to 20 mV/m and

its frequency to vary from 2 kHz. The angle of propagation has been taken to vary between zero to  $60^\circ$ .

Fig. 1 shows the variation of the growth rate and the real frequency for various values of the temperature anisotropy in the presence of the AC field  $E_0 = 20$  mV/m with a frequency of 2 kHz. It is observed that the growth rate increases by increasing the value of temperature anisotropy it means that it behaves like a free energy source. It is also observed that in the presence of AC field, the growth rate and also the bandwidth more increases in comparison to the case when the AC field is absent, this shows that the AC field has additive effect. Thus a minimum of electric field magnitude is enough to trigger the Whistler emission and the existing growth of the wave to a higher value, increasing the power by a few deci Bels in comparison to that without the AC signal. These triggered emissions have been observed by instruments on board satellites [15, 16] and if these emissions are ducting along the field lines they may be recorded by ground stations.

Fig. 2 shows the variation of growth rate and real frequency with respect to  $\bar{k}$  for various values of AC field frequency in the case when temperature anisotropy is 1.5. In this case it is observed that the growth rate and also the bandwidth increase with the increase of the AC field frequency. It shows that AC field frequency introduces a small growth and provides some free energy to make the plasma unstable sustaining the growth of Whistler waves.

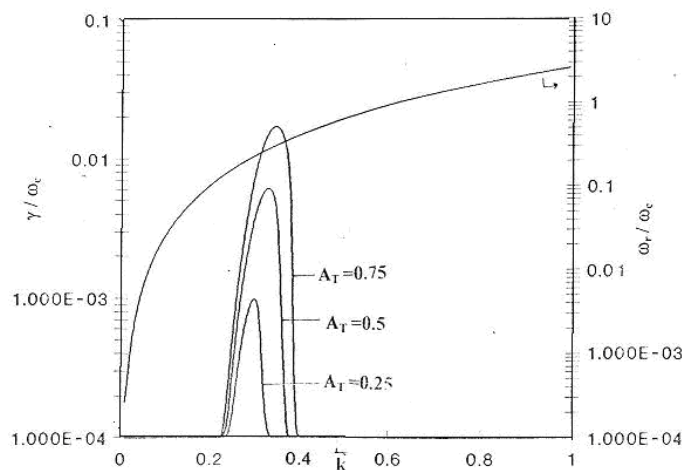


**Fig. 1: Variation of Growth rate and real frequency with respect  $\bar{k}$  to for various values of Temperature anisotropy at other fixed Plasma Parameters.**

In Fig. 3 the growth rate and real frequency is plotted against  $\bar{k}$  for various values of the loss-cone angle in the presence of temperature anisotropy for other fixed plasma parameters. It shows that with the increase of the loss-cone angle, the growth rate goes on increasing simultaneously increasing the bandwidth. This indicates that the loss cone angle is supposed to provide additional energy for generating Whistler wave of low frequencies.

Fig. 4 shows the variation of the growth rate and real frequency with  $\bar{k}$   $k$  for various values of the magnitude of the electron energy  $k_B T_{||}$ . It is observed that with the increase of the magnitude



of the electron energy, the growth rate increases and broadens the range of  $\bar{k}$ . That is emission is possible for extended values of  $\bar{k}$ . Fig. 5 shows the variation of growth rate and real frequency with  $\bar{k}$  for various values of angle of propagation. With the increase of the angle of propagation the growth rate increases slightly and the change in obliqueness broadens the wave spectrum over wide range. This is in agreement with the observation due to the change in resonance condition.

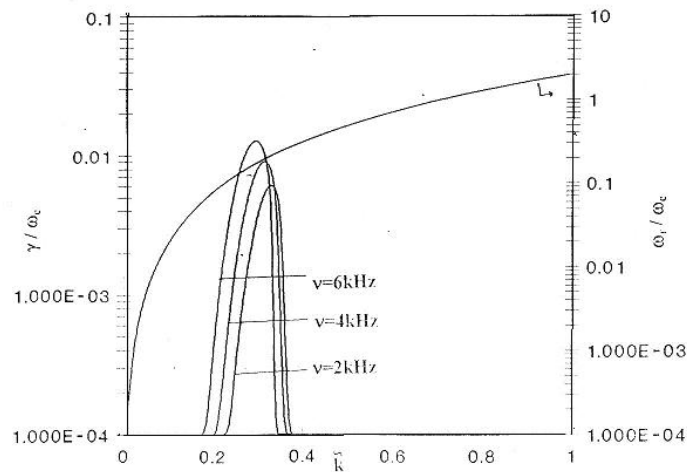


**Fig. 2: Variation of Growth rate and real frequency with respect  $\bar{k}$  to for various values of AC field frequency at other fixed Plasma Parameters.**

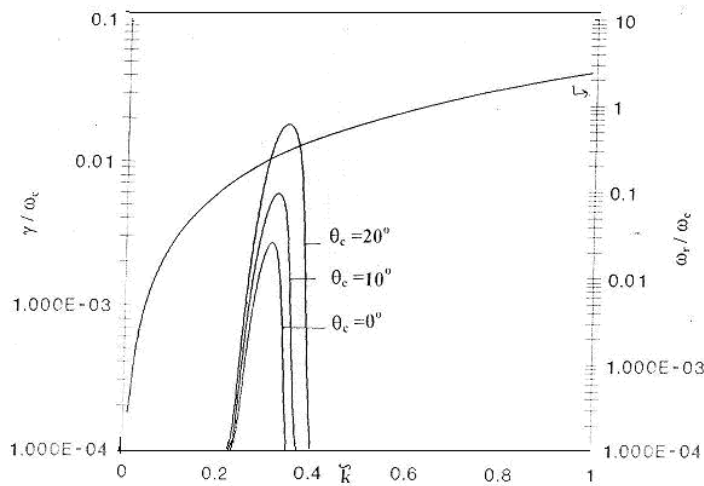


**Fig. 3: Variation of Growth rate and real frequency with respect  $\bar{k}$  to for various values of Loss-cone angle at other fixed Plasma Parameters.**

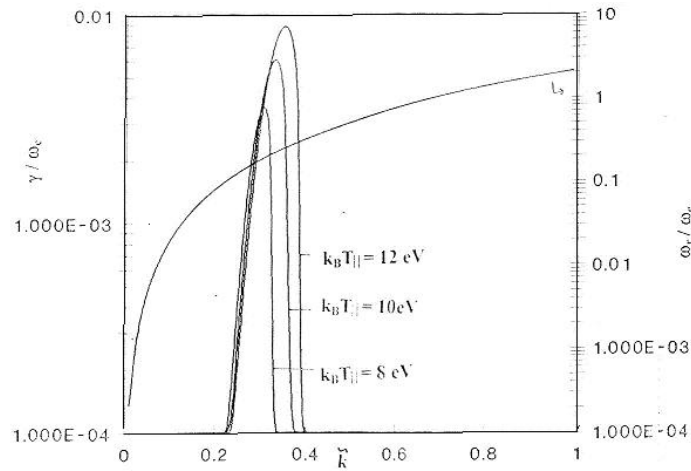


Fig. 4: Variation of Growth rate and real frequency with respect  $\tilde{k}$  to for various values of Electron energy  $K_B T$  at other fixed Plasma Parameters

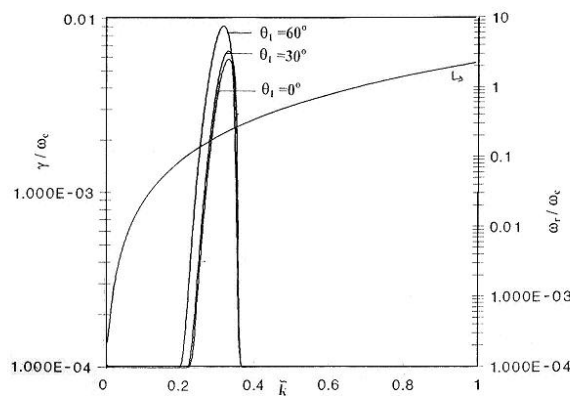


Fig. 5: Variation of Growth rate and real frequency with respect  $\tilde{k}$  to for various values of Angle of propagation at other fixed Plasma Parameters.

### REFERENCES

- [1] Scharer, J.E., *Phys. Fluids* 10, 652 (1967).
- [2] Cuperman, S., *Rev Geophys. Space Phys.* 19, 307 (1981).
- [3] Helliwell, R.A., *J. Geophys. Res.* 72, 4773 (1967).
- [4] Kennel, C.F. and H.E. Petschek, *J. Geophys. Res.* 71, 128 (1966).
- [5] Inan, U.S., T.F. Bell and R.A. Helliwell, *J. Geophys. Res.* 83, 3235 (1978).
- [6] Johnstone, A.D., *Ann. Geophys.* 41, 397 (1983).
- [7] Stenback-Nielson, H.C., *Geophys. Res. Lett.* 7, 353 (1980).
- [8] Oguti, T.R., *J. Geophys. Res.* 81, 1782 (1976).
- [9] Huang, L., J.G. Haukins and L.C. Lee, *Journal of Geophys. Res.* 95, 3893 (1990).
- [10] Pandey, R.P., K. M. Singh and R. S. Pandey, *Earth Moon and Planets* 87, 59 (2001).

- [11] Pandey, R.S., U. C. Srivastava, A. K. Srivastava, S. Kumar and D. K. Singh, *Archives of Physics Research*, 1(4),126-136, (2010).
- [12] Misra, K.D.and R.S. Pandey, *J. Geophys. Res.* 100, 1905 (1995).
- [13] Sazhin, S.S., *Planets. Space Sci.* 36, 663 (1988).
- [14] Pandey , R. S. and K.D. Misra, *Earth moon and space* (Japan) 54,159 (2002).
- [15] Inan, U.S., T.F. Bell and D.L. Carpenter, *J. Geophys. Res.* 82, 1177 (1977).
- [16] Bell, T.E., R.A. Helliwell, *ISEE trans. Geo sci. Elect.* GE-16 (1978).